Molecular Biology of the Cell
Vol. 20, 5086–5095, December 15, 2009

Phosphatidylserine Regulation of Ca^{2+}-triggered Exocytosis and Fusion Pores in PC12 Cells

Zhen Zhang,* Enfu Hui,†‡ Edwin R. Chapman,‡ and Meyer B. Jackson§

*Molecular and Cellular Pharmacology Graduate Program, †Program in Biophysics, ‡Howard Hughes Medical Institute, and §Department of Physiology, University of Wisconsin School of Public Health, Madison, WI 53706

Submitted August 14, 2009; Revised September 22, 2009; Accepted October 7, 2009
Monitoring Editor: Patrick J. Brennwald

The synaptic vesicle protein synaptotagmin I (Syt I) binds phosphatidylserine (PS) in a Ca^{2+}-dependent manner. This interaction is thought to play a role in exocytosis, but its precise functions remain unclear. To determine potential roles for Syt I-PS binding, we varied the PS content in PC12 cells and liposomes and studied the effects on the kinetics of exocytosis and Syt I binding in parallel. Raising PS produced a steeply nonlinear, saturating increase in Ca^{2+}-triggered fusion, and a graded slowing of the rate of fusion pore dilation. Ca^{2+}-Syt I bound liposomes more tightly as PS content was raised, with a steep increase in binding at low PS, and a further gradual increase at higher PS. These two phases in the PS dependence of Ca^{2+}-dependent Syt I binding to lipid may correspond to the two distinct and opposing kinetic effects of PS on exocytosis. PS influences exocytosis in two ways, enhancing an early step leading to fusion pore opening, and slowing a later step when fusion pores dilate. The possible relevance of these results to Ca^{2+}-triggered Syt I binding is discussed along with other possible roles of PS.

INTRODUCTION

Phosphatidylserine (PS) is an abundant anionic phospholipid with many roles in cell signaling and membrane trafficking (Stace and Ktistakis, 2006). Synaptotagmin I (Syt I) is a PS-binding protein on synaptic vesicles that serves as a Ca^{2+} sensor in neurotransmitter release at synapses (Augustine, 2001; Chapman, 2002; Koh and Bellen, 2003). Syt I binds to PS-containing liposomes in a Ca^{2+}-dependent manner (Brose *et al*., 1992), and this interaction, along with Ca^{2+}-dependent Syt I interactions with soluble *N*-ethylmaleimide sensitive factor attachment protein receptors (SNAREs) and other effectors are thought to play critical roles in exocytosis (Chapman, 2002; Brunger, 2005). A great deal of functional mutagenesis work has been undertaken to elucidate the mechanism by which Syt I triggers exocytosis and to determine the specific roles of Ca^{2+}-triggered binding of Syt I to PS and SNAREs (Fernandez-Chacon *et al*., 2001, 2002; Mackler *et al*., 2002; Stevens and Sullivan, 2003; Wang *et al*., 2003a,b; Bai *et al*., 2004; Nishiki and Augustine, 2004; Pang *et al*., 2006; Wang *et al*., 2006; Lynch *et al*., 2008; Paddock *et al*., 2008). However, these studies have failed to produce a clear consensus, partly because of difficulties in finding mutations that selectively alter Syt I binding to various effectors, and partly because of inconsistencies in the literature.

This article was published online ahead of print in *MBC in Press* (http://www.molbiolcell.org/cgi/doi/10.1091/mbc.E09–08–0691) on October 14, 2009.

Address correspondence to: Meyer B. Jackson (mjackson@physiology.wisc.edu).

Abbreviations used: FRET, fluorescence resonance energy transfer; PS, phosphatidylserine; PSF, prespike foot; PSS, phosphatidylserine synthase.

In view of the difficulty of resolving the functional roles of Syt I–effector interactions in exocytosis, it would be useful to have an independent test of the functions of the binding partners of Syt I. It is well established that the SNARE proteins are essential for exocytosis at synapses (Sollner *et al*., 1993; Jahn and Scheller, 2006). Although PS is essential for Ca^{2+}-Syt I stimulated liposome fusion (Bhalla *et al*., 2005), its role in exocytosis has not been as clearly established as that of SNARE proteins. To address the role of PS independently of Syt I, we manipulated PS levels in neuroendocrine PC12 cells, either by adding PS to the culture medium or by expressing various forms of the enzyme PS synthase (PSS). We then used amperometry to evaluate the functional consequences. Parallel studies of the PS dependence of Ca^{2+}-triggered binding of Syt I to lipids allowed us to compare the actions of PS in living cells to the Syt I–PS interaction in vitro.

Exocytosis can be resolved into a sequence of steps such as vesicle docking, priming, fusion pore opening, and fusion pore dilation. Amperometry recording has shown that Syt isoforms and mutations alter the lifetime of fusion pores (Wang *et al*., 2001, 2003a, 2006; Bai *et al*., 2004), and capacitance recording has shown that varying the expression of Syt I and Syt II alters the relative amounts of rapid and slow release (Nagy *et al*., 2006). Mutations in the lipid penetrating loops alter the dilation of fusion pores (Lynch *et al*., 2008). The fact that Ca^{2+} accelerates both fusion pore opening and fusion pore dilation raises the possibility that different Syt I–effector interactions mediate distinct kinetic steps in exocytosis (Wang *et al*., 2006). The amperometry data reported here has enabled us to resolve PS effects on distinct kinetic steps during Ca^{2+}-triggered fusion. On the basis of these results, we propose that PS influences the opening of fusion pores as well as their subsequent dilation. We discuss the possibility that these processes represent loci at which Ca^{2+}-triggered Syt binding to PS could drive Ca^{2+}-triggered exocytosis.

MATERIALS AND METHODS

Amperometry

Norepinephrine release was recorded with a VA-10 amperometry amplifier (ALA Scientific, Westbury, NY) by using 5-μm carbon fiber electrodes held at 650 mV (Zhang and Jackson, 2008). Cells were bathed in a solution containing 150 mM NaCl, 4.2 mM KCl, 1 mM NaH_2PO_4, 0.7 mM $MgCl_2$, 2 mM $CaCl_2$, and 10 mM HEPES, pH 7.4. Secretion was evoked by pressure application of a solution identical to the bathing solution, but with 105 mM KCl and 5 mM NaCl. This solution was applied from a ~1-μm micropipette with 6-s pressure pulses (10–20 PSI) from a Picospritzer (Parker-Hannefin, Cleveland, OH).

Amperometry spikes and prespike feet (PSF) were analyzed as described previously (Zhang and Jackson, 2008). Cumulative spike counts were based on spikes with peak amplitudes ≥2 pA and were plotted versus time at intervals of 250 ms. Spike frequency was obtained as the total number of spikes recorded for 20 s after the start of depolarization, divided by 20 s. PSF were measured for spikes with amplitudes ≥20 pA. Large kiss-and-run events (as distinct from small kiss-and-run events; Wang *et al*., 2003a) were recognized by their rectangular shape and amplitude between 2 and 3.5 pA (Wang *et al*., 2006). The Student's *t* test was used to determine statistical significance from averages over cells.

Plasmid Construction and Cell Culture

cDNAs encoding PSS1 and PSS2 were kindly provided by Dr. Jean Vance at University of Alberta, Edmonton, AB, Canada. The gain of function mutations, PSS1-R95K and PSS2-R97K (Kuge and Nishijima, 2003), were generated using QuikChange site-directed mutagenesis polymerase chain reaction (PCR) (Stratagene, La Jolla, CA). PSS1, PSS1-R95K, PSS2, and PSS2-R97K were cloned into the pCDNA3.1 vector. Syt I C2AB was cloned into the pGEX-2t vector and expressed as described below for cosedimentation and stopped-flow experiments. All constructs were verified by sequencing.

Methods of cell culture follow previous reports from this laboratory (Han and Jackson, 2006; Wang *et al*., 2006). PC12 cells were cultured at 37°C in a humidified incubator with a 10% CO_2/air atmosphere. Cells were plated into dishes coated with collagen I (BD Biosciences, San Jose, CA) and poly-D-lysine (Sigma-Aldrich, St. Louis, MO) and loaded with 1.5 mM norepinephrine and 0.5 mM ascorbate 14–16 h before experiments. Phospholipids were added from a dimethyl sulfoxide (DMSO) stock solution to the culture medium 2 d before recording. Final DMSO was 0.1%, and control recordings were treated with 0.1% DMSO only.

Stable Cell Line Generation

PC12 cells were transfected with designated PSS constructs by using Lipofectamine 2000 (Invitrogen, Carlsbad, CA). About 16 h after transfection, medium was changed to complete medium supplemented with 0.5 g/l neomycin (Invitrogen). The medium was changed every day for 7–10 d until all nontransfected cells had died. Cells were split into 96-well plates to allow 1–2 cells/well and grown for ~2 wk to get stable transfected cell lines. Positive clones were identified by reverse transcription-PCR (data not shown). Phospholipids were extracted (Folch *et al*., 1957) and analyzed by high-performance liquid chromatography (HPLC) with a silica column (Van Kessel *et al*., 1977) (see Supplemental Data).

Protein Expression and Purification

The cytoplasmic domain of Syt I (designated as syt I C2AB, residues 96-421) was generated as glutathione transferase (GST) fusion protein using pGEX-2T vector. *Escherichia coli* were grown at 37°C to an OD_{600} of 0.8, and protein expression was induced with 0.4 mM isopropyl β-D-thiogalactoside. Four hours after induction, the bacteria were collected by centrifugation, and the pellet was resuspended in HBS (100 mM NaCl and 25 mM HEPES, pH 7.4) containing 1 mM dithiothreitol (DTT). Bacteria were sonicated and treated with Triton X-100 and protease inhibitors. The supernatant was collected following centrifugation and incubated with rotation overnight with glutathione-Sepharose beads at 4°C. Recombinant Syt I harbors tightly bound nucleic acid contaminants that may alter its biochemical properties (Ubach *et al*., 2001). To remove these contaminants, beads were washed two times with wash buffer (1 M NaCl and 25 mM HEPES, pH 7.4, 1 mM DTT, and 0.1 mg/ml RNase and DNase) and another two times with regular HBS. The GST tag was removed by thrombin cleavage (50 U/ml bead slurry for 2 h at 22°C), and the supernatant was treated with phenylmethylsulfonyl fluoride to inactivate the thrombin. Syt I C2AB protein was subjected to SDS-polyacrylamide gel electrophoresis (PAGE) and stained with Coomassie Blue to determine concentration against a bovine serum albumin standard curve. Removal of bacterial contaminants was confirmed by measuring the UV spectrum of the purified protein (Ubach *et al*., 2001).

Liposomes

Chloroform solutions of dioleoylphosphatidylcholine and dioleoylphosphatidylserine (Avanti Polar Lipids, Alabaster, AL) were mixed in the desired proportion, dried first under nitrogen, and then under vacuum. Dried lipids were resuspended in HBS, and the suspensions passed through 100- or 400-nm polycarbonate filters to generate liposomes with a mean diameter of ~138 or ~252 nm, respectively (Hui *et al*., 2009). Starting with the conversion for 100-nm liposomes of 1 mM lipid = 11 nM liposome (Bai *et al*., 2002), [liposome] was calculated from [lipid] as follows: for 138-nm liposomes, 1 mM lipid = 11× ($100^2/138^2$) nM liposome = 5.78 nM liposome; and for 252-nm liposomes, 1 mM lipid = 11× ($100^2/252^2$) nM liposome = 1.73 nM liposome.

Cosedimentation Assay

Protein (0.35 nmol) was incubated with a designated concentration of liposomes (252 nm in diameter) in the presence of 1 mM Ca^{2+} or 0.2 mM EGTA for 15 min at 22°C. The mixture was centrifuged for 40 min at 65,000 × *g* at 4°C. Supernatant was subjected to SDS-PAGE, stained with Coomassie Blue, and analyzed using ImageJ software (National Institutes of Health, Bethesda, MD). Bound protein was expressed as a percentage of the total input.

Stopped-Flow Kinetics Experiments

The kinetics of Ca^{2+}-dependent Syt I C2AB binding to PS-containing liposomes (~138 nm in diameter) was monitored by fluorescence resonance energy transfer (FRET) by using an SX.18MV stopped-flow spectrometer (Applied Photophysics, Surrey, United Kingdom) as described previously (Bai *et al*., 2004). The aromatic residues in the Syt I C2AB domain were excited at 285 nm and served as energy donors for dansyl groups attached to the phospholipid headgroups. Dansyl emission was selected using a 470-nm cut-off filter. The on-rate (k_{on}), off-rate (k_{off}), and dissociation constant ($K_{D\text{-}sf}$) for the C2AB liposome interaction are related by the following equations. $k_{obs} = [\text{liposome}]k_{on} + k_{off}$ and $k_{D\text{-}sf} = k_{off}/k_{on}$.

Lipid Extraction from PC12 Cells

Total lipids were extracted from cells (10^6 cells in 1 ml) by using a modified Folch procedure (Folch *et al*., 1957). Methanol (2 ml) containing butylated hydroxytoluene (0.1 mg) was added to the cell suspension and mixed. Chloroform (4 ml) was added and the mixture was stored for 1 h at 4°C under N_2. One milliliter of 0.1 M NaCl was added, and the mixture was vortexed under nitrogen. After centrifugation for 5 min at 1500 × *g*, the lower chloroform layer was transferred to a new tube and evaporated to dryness under a stream of nitrogen. The lipid extract was dissolved in 0.2 ml of chloroform.

HPLC Analysis of Cell Lipids

Lipid extracts were resolved with a high-performance liquid chromatograph (System Gold, 168 Detector, 126 Solvent Module; Beckman Coulter, Fullerton, CA) (Van Kessel *et al*., 1977). The lipid extracts were applied to a 5-mm Supelcosil LC-Si column (25 cm × 4.6 mm) equilibrated with solvent B1 (2-propanol:hexane:water [6:2:1.5]). The column was eluted during the first 0–5 min with solvent A (2-propanol:hexane:water [58:40:2]), 5–20 min with a liner gradient to 100% solvent B2 (2-propanol:hexane:water [58:40:8]), and finally 20- to 40-min isocratic with 100% solvent B2. The solvent flow rate was maintained at 1 ml/min. The effluent was monitored by absorbance at 206 nm. Data were collected with 32 Karat software (Beckman Coulter). The identities of phospholipids in the chromatogram were established by running lipid standards (Avanti Polar Lipids) under the same conditions.

Extraction of plasma membrane lipids follows previous reports (Scott, 1976; Perkins and Scott, 1978), with modification. In brief, PC12 cells grown to 75% confluence were washed three times in 4 ml of phosphate-buffered saline, pH 7.4, containing 0.75 mM Ca^{2+} and 0.5 mM Mg^{2+} (phosphate-buffered saline [PBS] wash). Cells were then incubated with 5 ml of washing buffer supplemented with 25 mM formaldehyde and 2 mM dithiothreitol for 2 h at 37°C to shed plasma membrane vesicles. The vesiculant solution was collected and centrifuged at 25,000 × g for 1 h at 4°C. The pellet was washed three times with PBS. The final plasma membrane pellet was used to extract lipids by the Folch chloroform-methanol method described above.

RESULTS

PS Effects on Exocytosis

As an initial attempt to test the role of PS in exocytosis, we added 100 μM PS directly to the culture medium (Uchiyama *et al*., 2007). Two days later, lipid analysis with HPLC showed that this raised the total PS content of PC12 cells from 10.3 to 12.1% (Table 1). Amperometry was then used to measure norepinephrine release from single PC12 cells, by using KCl depolarization to trigger exocytosis (Figure 1A). The cumulative spike-counts are plotted versus time in Figure 1B. These recordings showed that PS addition produced a statistically insignificant increase in the frequency of Ca^{2+}-triggered vesicle fusion events by 22%, from 1.60 ± 0.16 to 1.96 ± 0.19 spikes/s ($p = 0.15$).

Table 1. PS content of PC12 cells

Cell condition	PS content (%)
Control	10.3 ± 0.7
Control + 100 μM PC	9.9 ± 0.7
Control + 100 μM PS	12.1 ± 0.5
PSS2	13.5 ± 0.7
PSS1	14.7 ± 0.2
PSS1-R95K	15.4 ± 0.5
PSS2-R97K	16.1 ± 0.7
PSS2 + 100 μM PS	19.0 ± 1.9
PSS1 + 100 μM PS	21.0 ± 2.8
PSS1-R95K + 100 μM PS	28.1 ± 1.0
PSS2-R97K + 100 μM PS	30.0 ± 0.4

PS content was determined by HPLC for PC12 cells with added PS/PC and/or expressing the various forms of PSS. All conditions included 0.1% DMSO for 1 d before recording.

The full fusion of a vesicle registers as a spike in an amperometry recording, with a PSF signaling the opening of a fusion pore (insets in Figure 1A). PSF have approximately exponential lifetime distributions, and exponential fits to these distributions provide the mean fusion pore lifetime (Figure 1C). The PSF lifetime was significantly longer in PS-treated PC12 cells (1.55 ± 0.08 vs. 1.19 ± 0.09 ms; $p < 0.01$) (Figure 1D), suggesting that increasing the membrane PS content stabilizes open fusion pores. This effect was specific to PS; addition of 100 μM phosphatidylcholine (PC) failed to alter vesicle fusion event frequency (1.53 ± 0.15 spikes/s, $p = 0.9$) and fusion pore lifetime (1.14 ± 0.04 ms, $p = 0.9$). Note that PC addition did not significantly alter the PS content (Table 1).

Based on these initial results, we sought to study the effect of varying cellular PS content more thoroughly. To increase its biosynthesis, we used cDNAs encoding two different isoforms of PS synthase (PSS1 and PSS2), as well as their gain-of-function mutants (PSS1-R95K and PSS2-R97K), to generate stably transfected PC12 cell lines. PSS1 exchanges the choline of phosphatidylcholine for serine (Kuge *et al*., 1985; Voelker and Frazier, 1986), whereas PSS2 exchanges the ethanolamine of phosphatidylethanolamine for serine (Kuge *et al*., 1997; Saito *et al*., 1998). PSS1-R95K and PSS2-R97K are resistant to the inhibitory regulation of enzyme activity and therefore can elevate PS to higher levels than the wild-type enzymes (Kuge and Nishijima, 2003). In combination with the addition of exogenous PS to the culture medium described above, these various manipulations allowed us to achieve 11 different conditions. HPLC of total cellular lipids indicated that the various conditions produced PS content ranging from 10 to 30% (Table 1 and Supplemental Figure S1A for a sample HPLC trace used to quantitate phospholipids). In PSS1 and PSS1-R95K stably transfected cell lines, PC content decreased as PS content rose with a

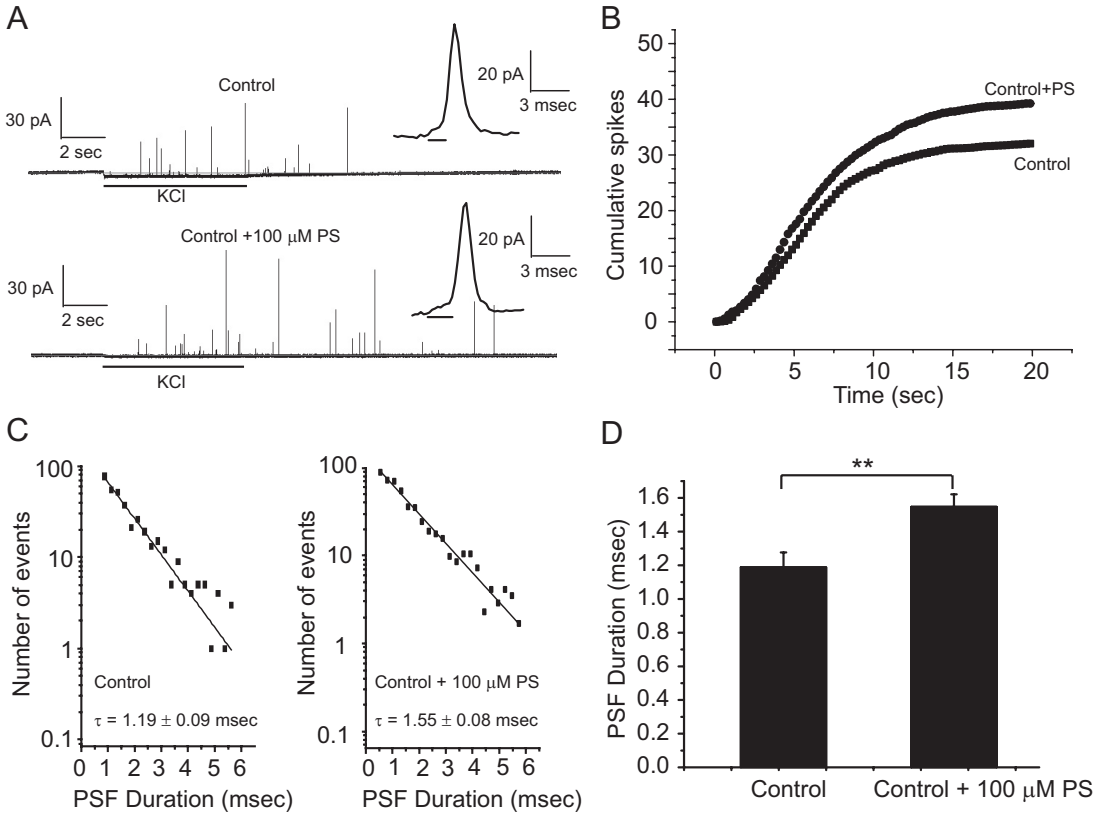

Figure 1. Secretion rate and fusion pore stability are increased by PS addition to the cell culture medium. (A) Amperometry traces from vehicle control (0.1% DMSO) or 100 μM PS-treated PC12 cells. Secretion was elicited by KCl depolarization for 6 s (indicated by the bars below each trace). Expanded traces show representative spikes with PSF in each inset. (B) Plot of cumulative spike count versus time shows the frequency of vesicle fusion events per cell. (C) PSF lifetime distribution for control and 100 μM PS-treated PC12 cells. Data from 752 spikes and 42 cells for control; 844 spikes and 43 cells for PS. (D) Mean PSF duration for control PC12 cells and 100 μM PS; 752 spikes with PSF for control and 844 spikes with PSF for PS-treated PC12 cells. **$p < 0.01$. Error bars represent SEM.

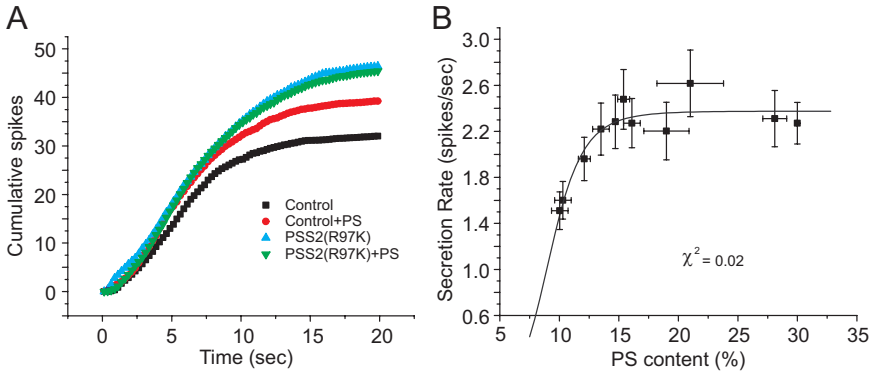

Figure 2. Both endogenous and exogenous PS increase secretion. (A) Plot of vesicle fusion frequency versus PS content in PC12 cells with best-fitting Hill equation. Control and +PS plots are from Figure 1B. (B) Cumulative spike frequency plots for control and for selected conditions of elevated PS. Data from 37 to 47 cells for each PS content. Error bars represent SEM.

slope of −0.50 (Supplemental Figure S1B). A similar trend was found with PSS2 and PSS2-R97K stably transfected cell lines, where PE content decreased as PS content rose with a slope of −0.09 (Supplemental Figure S1C). These data suggest that rises in PS are greater than the declines in the respective biosynthetic precursors, as expected from the compensatory mechanisms that cells employ to maintain phospholipid levels (Vance and Vance, 2004). Because each of these forms of PSS elevate PS with different compensatory changes in the amounts of the biosynthetic precursors PE and PC, these results indicate that we can distinguish the effects of PS from the effects of PE and PC.

To check the distribution of PS in the plasma membrane and in intracellular membranes we isolated plasma membrane from PC12 cells, extracted lipids, and analyzed lipid composition by HPLC. Selecting control PC12 cells, PSS2-R97K cells, and PSS2-R97K+PS cells as representative examples with widely varying total PS contents, the PS in the plasma membrane was indistinguishable from the PS of total lipids (Supplemental Figure S1D). HPLC measures percent of total lipid, but PS is essentially absent from the outer leaflet of the plasma membrane (Pomorski *et al.*, 2001; Daleke, 2003). To check that PS increments do not overflow to the outer leaflet, we used a confocal microscope and the PS fluorescent probe annexin-V-fluorescein isothiocyanate (FITC) to localize PS (Yeung *et al.*, 2006) in control cells, PSS2-R97K cells, and PSS2-R97K+PS cells. In intact cells, annexin-V-FITC failed to stain any of these three types of cells, confirming that PS is absent from the outer leaflet of the cell membrane (Supplemental Figure S1E). To reveal PS content in the inner leaflet of the cell membrane, cells were treated with ionomycin to activate the membrane scramblase (Zwaal *et al.*, 2005) and flip PS from the inner leaflet to the outer leaflet of the cell membrane. After ionomycin treatment all three cell variants presented fluorescence upon staining with annexin-V-FITC (Supplemental Figure S1E). PSS2-R97K+PS PC12 cells had the brightest fluorescence, indicating these cells had the highest level of PS in the inner leaflets of their plasma membrane. This is consistent with the highest PS levels seen with HPLC (Table 1). To reveal all of the PS, cells were fixed in paraformaldehyde and permeabilized with 0.3% Triton X-100. PSS2-R97K+PS cells again exhibited the brightest annexin-V-FITC staining. Together, the HPLC measurements and annexin-V-FITC staining experiments showed that PS content was elevated by the various manipulations, and as levels changed, PS remained concentrated in the inner leaflet of the plasma membrane. Because PS content was the same in the plasma membrane and total cell lipids (Supplemental Figure S1D), we can take the PS content of the inner leaflet of the plasma membrane as double that in Table 1.

Amperometry recording showed that the secretion rate increased with higher PS content (Figure 2A). The plot of secretion rate versus PS content was fitted to the Hill equation, yielding V_{max} = 2.38 ± 0.07 spikes/s, EC_{50} = 9.15 ± 0.40%, and n (the Hill coefficient) = 6.49 ± 2.13, χ^2 = 0.02 (Figure 2B). Constraining n to a value of one gave a much poorer fit (χ^2 = 0.06). Thus, as PS content rose exocytosis increased very steeply, indicating a highly cooperative interaction. The effect of PS saturated at high PS content, and it is difficult to determine whether this plateau reflects a limit due to the size of a releasable vesicle pool (Sorensen, 2004), a change in which step is rate limiting, or saturation of the rate of Syt-PS binding.

The kinetics of exocytosis can be influenced by many factors. It is known that both cytoplasmic Ca^{2+} (Wang *et al.*, 2006) and vesicle size (Sombers *et al.*, 2004; Amatore *et al.*, 2005; Zhang and Jackson, unpublished) alter fusion pore dynamics. This raises the question of whether PS levels change exocytosis indirectly by altering Ca^{2+} current, vesicle size or number, or by altering the levels of other exocytosis proteins. Whole-cell patch clamp showed that PS levels failed to alter Ca^{2+} current (Supplemental Figure S3) and electron microscopy showed that altering PS levels had no impact on vesicle size or number (Supplemental Figure S4). Western blots showed that elevating PS did not alter the levels of synaptobrevin, synaptosomal-associated protein of 25 kDa, syntaxin 1A, syntaxin 1B, or Syt I (Supplemental Figure S5). Thus, the kinetic changes in exocytosis resulting from elevated PS levels are unlikely to reflect an indirect action of PS on Ca^{2+} channels, or vesicle size or number, or the levels of some of the major exocytosis proteins.

Fusion pore lifetimes also increased with higher PS content (Figure 3A). In contrast to the secretion rate, this plot showed no saturation but was linear through the entire range of PS content (R^2 = 0.94, $p < 0.001$) (Figure 3B). PSF amplitude, which reflects the rate of norepinephrine flux through the initial fusion pore, showed no dependence on PS content (Supplemental Figure S2F). Once dilation has started the shape of a spike reflects the rate of norepinephrine efflux through an expanding fusion pore and diffusion to the carbon fiber electrode. (Comparison of spike kinetics with diffusion models have shown that norepinephrine dissociation from the granule matrix is not rate limiting in these cells; Zhang and Jackson, 2008.) We analyzed spike amplitude, rise time, decay time, half width, and total area, and found that plots of these quantities versus PS content were flat with no significant dependence on PS (Supplemental Figures S2, A–E). Thus, PS has no effect on these late kinetic steps that determine spike shape. It remains possible that PS could influence the rate of fusion pore expansion as this rate

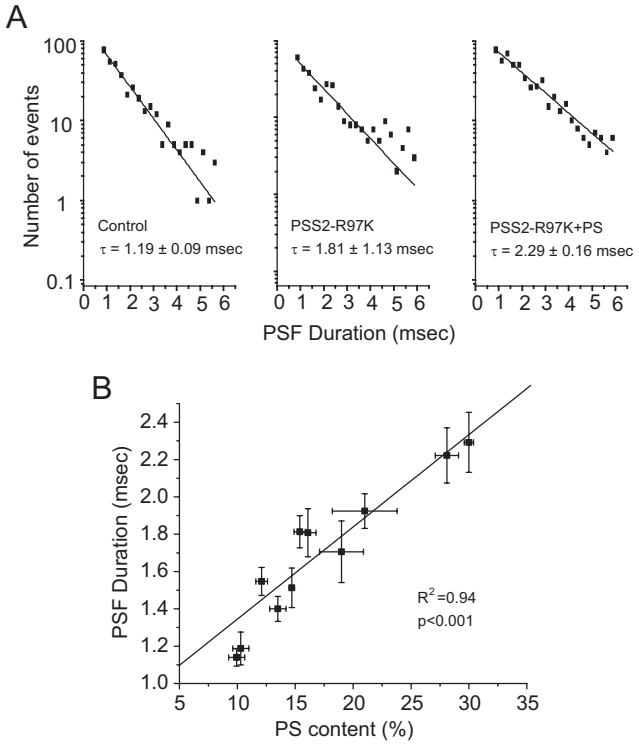

Figure 3. PS increases fusion pore lifetime. (A) PSF lifetime distributions for control PC12 cells, PSS2-R97K stably transfected PC12 cells, and PSS2-R97K stably transfected PC12 cells treated with 100 μM PS. (B) Plot of PSF lifetime versus PS content together with the best-fitting line. Data are from 319 to 960 PSF for each point.

is probably too fast to be rate limiting in the diffusion of norepinephrine to the carbon fiber electrode.

To probe the effect of PS on fusion pores in greater detail, we analyzed kiss-and-run events in which fusion pore openings do not resolve to spikes. Assuming that an open state can convert to either a closed state with a rate constant k_c or a dilating state with rate constant k_d allows one to calculate these two rate constants. With a measurement of fusion pore lifetime as $\tau = 1/(k_c + k_d)$, together with a measurement of the fraction of kiss-and-run events as $X_{KR} = k_c/(k_c + k_d)$ we can solve for k_c and k_d (Wang *et al*., 2006). X_{KR} showed a small, statistically insignificant increase with elevated PS content ($p = 0.40$, slope = 0.002) (Figure 4A). k_c decreased slightly with increasing PS content, but this change was also statistically insignificant ($p = 0.07$, slope = -0.004) (Figure 4B). Thus, PS has little if any effect on fusion pore closure. By contrast, k_d showed a strong and statistically significant decrease with increasing PS content ($p < 0.001$, slope = -0.015) (Figure 4C). Thus, PS stabilizes the open state of the fusion pore mainly by retarding the process of fusion pore dilation.

Syt–PS Interactions

To explore a possible relation between the effects of PS on exocytosis and Ca^{2+}-stimulated Syt I binding to lipid bilayers, we investigated Syt I binding to liposomes with a range of PS content. Selecting Syt I because it is the most abundant Syt isoform in PC12 cells (Tucker *et al*., 2003), we used cosedimentation to measure equilibrium binding of Syt I to liposomes with varying PS content. Increasing the PS content strengthened Syt I binding (in 1 mM Ca^{2+}) (Figure 5). The cosedimentation dissociation constant, $K_{D\text{-}cs}$, decreased by 3.5-fold as PS content increased from 10 to 12.5%. By contrast to this very steep change, increasing PS content further, up to 25%, produced a smooth decline in $K_{D\text{-}cs}$ that was well described by a single exponential ($p < 0.001$) (Figure 5, C and D). The exponential dependence of $K_{D\text{-}cs}$ implies a linear dependence of binding energy on PS content.

We then turned to stopped-flow kinetics to compare with the cosedimentation results as well as to investigate the kinetics of the interaction. The Syt I cytoplasmic domain (C2AB) was loaded into one syringe and PS-containing liposomes premixed with Ca^{2+} were loaded into another syringe of a stopped-flow apparatus. The lipid mixture contained a dansyl label that can be excited through a FRET interaction with aromatic residues in Syt I (Bai *et al*., 2002). Measuring dansyl emission thus provides a real-time readout of the Syt I–lipid interaction. Immediately after mixing (dead time, ~1 ms), fluorescence rose rapidly (Figure 6A). Single exponential fits to the fluorescence time course yielded observed rates (k_{obs}) that were then plotted against lipid concentration (Figure 6B). The slope of the fitted line yielded the on-rate (k_{on}), and the *y*-intercept yielded the off-rate (k_{off}) for the interaction of Ca^{2+}-C2AB with liposomes. The stopped-flow dissociation constant ($K_{D\text{-}sf}$) was calculated as k_{off}/k_{on}.

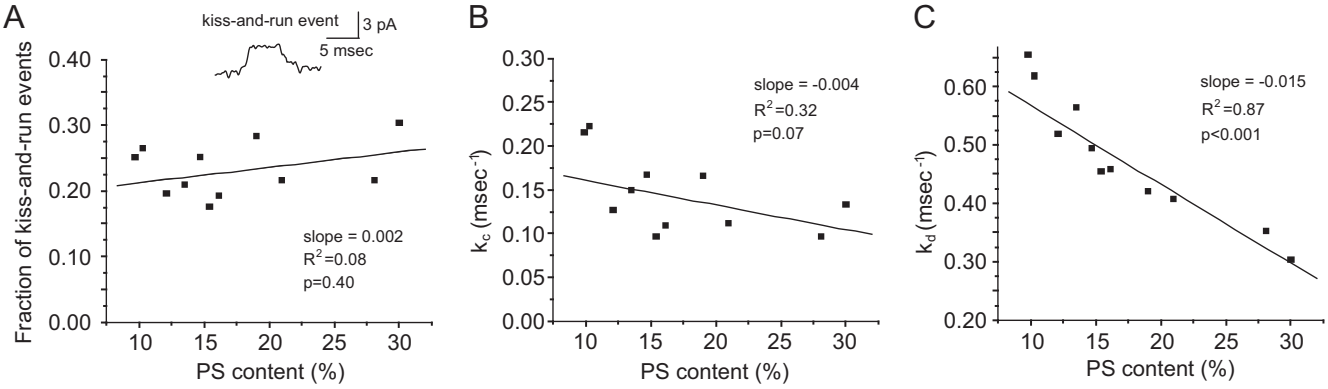

Figure 4. PS effects on fusion pore rate constants. (A) Plot of fraction of kiss-and-run events versus PS content shows no statistically significant dependence. A representative kiss-and-run event is shown in the inset. (B) Plot of k_c versus PS content shows no statistically significant dependence. (C) Plot of k_d versus PS content shows a statistically significant decrease with increasing PS content.

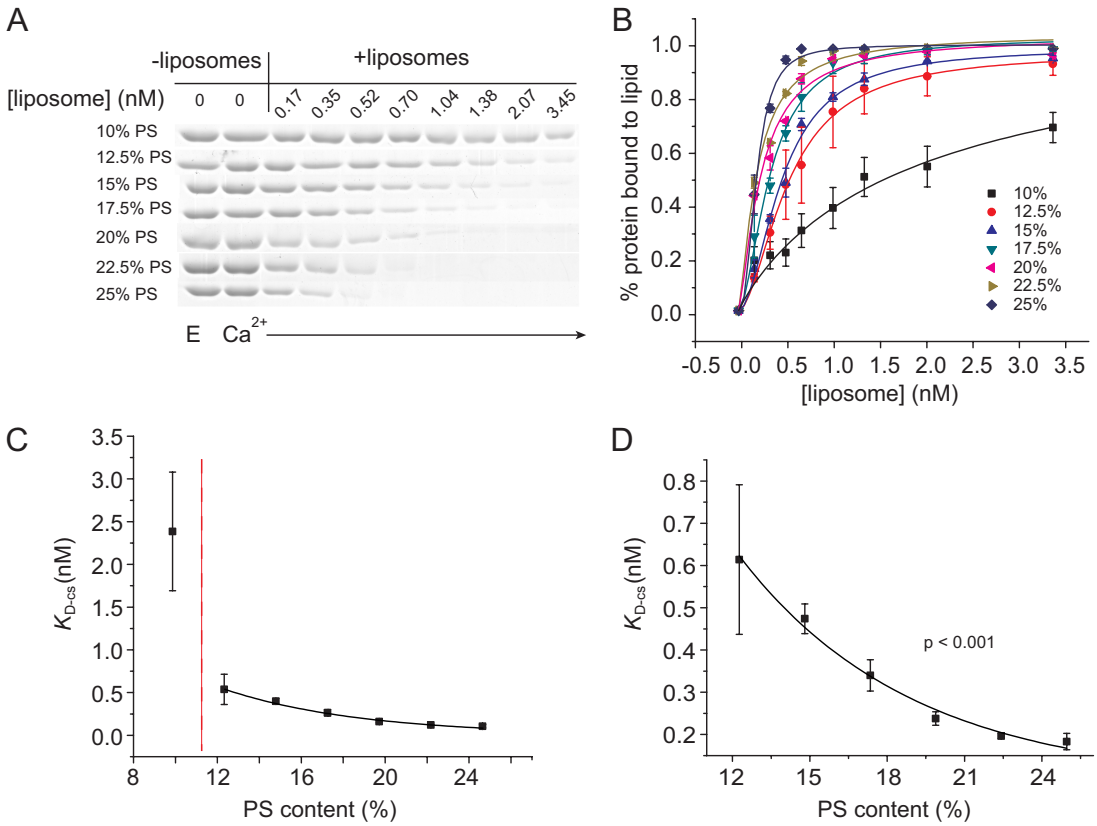

Figure 5. Syt I binding to PS-containing liposomes measured by cosedimentation. (A) A cosedimentation gel for Syt I bound to liposomes with PS content varied from 10 to 25% ([Ca^{2+}] = 1 mM). (B) Plot of percentage of protein bound to PS-containing liposomes versus [liposome]. (C) Plot of $K_{D\text{-}cs}$ versus PS content. (D) Plot as in C, but expanding the *y*-axis. The solid curve is the best-fitting exponential. Data are from three independent experiments. ***p < 0.001. Error bars represent SEM.

The rate and equilibrium constants are summarized in Table 2 and Figure 6C. It should be noted that cosedimentation and stopped-flow yield different values for the dissociation constant. For 15% PS, $K_{D\text{-}cs}$ = 0.48 ± 0.03 nM and $K_{D\text{-}sf}$ = 2.02 ± 0.81 nM (calculated on the basis of moles of liposome); for 25% PS, $K_{D\text{-}cs}$ = 0.19 ± 0.02 nM and $K_{D\text{-}sf}$ = 0.46 ± 0.29 nM. These differences partly reflect an effect of bilayer curvature: the cosedimentation experiments were performed on 252-nm liposomes and the stopped-flow experiments were performed on 138 nm liposomes. Furthermore, a slow step following the initial association contributes to the differences between these measurements. For a discussion of these issues in K_D measurements, see Hui *et al.* (2009). Despite these differences, $K_{D\text{-}sf}$ showed the same sharp drop as PS content increased from 9 to 12% as $K_{D\text{-}cs}$ (Figure 6D) (binding could not be detected at 6% PS). These results demonstrate that increasing the PS content of liposomes enhances Ca^{2+}-dependent Syt I binding, and this enhancement by PS exhibits two distinct phases.

DISCUSSION

This study has investigated the role of PS in Ca^{2+}-triggered exocytosis with the goal of evaluating kinetic steps that are influenced by PS. We varied the PS content of PC12 cells by adding PS to the culture medium and by expressing various forms of PS synthase. Each of these manipulations elevated PS while producing different compensatory reductions in other phospholipids. Plots of exocytosis versus PS content fell along a single curve, even though PC and PE varied differently for these conditions. Furthermore, PC addition had no effect, so we can attribute the changes in fusion event frequency and fusion pore dilation to changes in PS rather than changes in other phospholipids. Increasing PS levels left vesicle size and number, Ca^{2+} current, and levels of key exocytosis proteins unchanged (Supplemental Data). These experiments thus make a strong case for a direct functional role for PS in exocytosis.

Although this study has demonstrated that PS has effects on exocytosis, the mechanisms of these effects are not clear. The kinetic changes in exocytosis could reflect any of the following processes: 1) enhancement of Ca^{2+}-triggered Syt I binding to membranes; 2) enhancement of an interaction with another PS-binding protein involved in exocytosis; or 3) an effect of PS on physical properties of lipid bilayers, such as surface charge and spontaneous curvature. The enhancement of Syt I binding to membranes is appealing given the role of Syt I as a Ca^{2+} sensor for exocytosis (Augustine, 2001; Chapman, 2002; Koh and Bellen, 2003). The present study explored the PS dependence of Syt I binding in detail by using two different physical methods. We found that binding in vitro showed significant parallels with the enhancement of exocytosis by PS. However, the present study did not directly test the hypothesis that Ca^{2+}-dependent Syt I binding to membranes functions in exocytosis, and the present data to not allow us to make that conclusion. Indeed, because PS influenced both event frequency and fusion pore

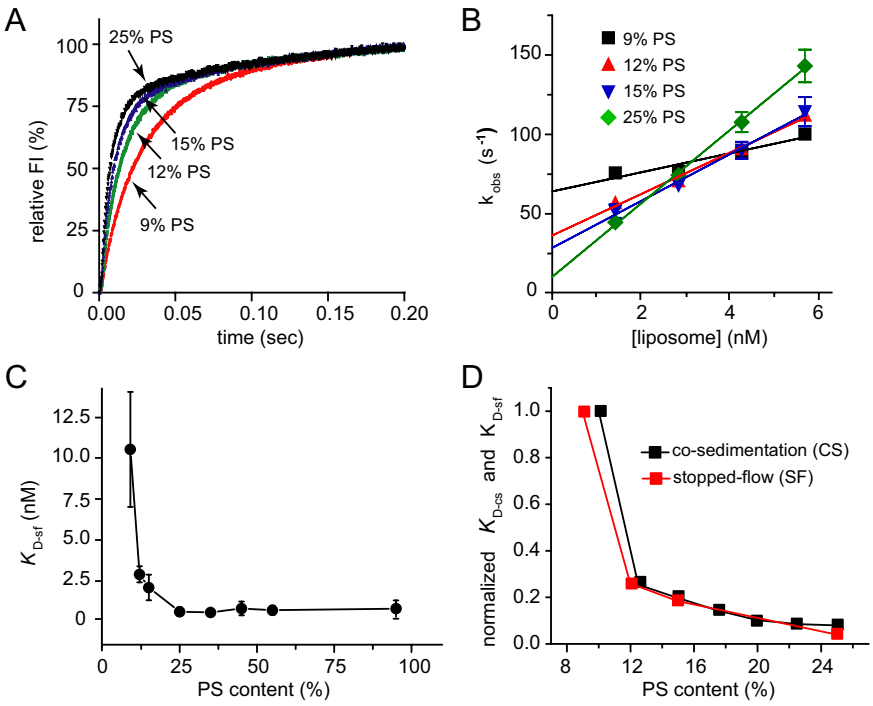

Figure 6. Kinetics of Syt I C2AB domain binding to PS-containing liposomes. (A) Sample traces of fluorescence signals for mixing of Syt I-C2AB and liposomes + Ca^{2+}. (B) k_{obs}, from exponential fits to traces in A, was plotted versus lipid concentration. (C) Dissociation constants ($K_{D\text{-}sf}$) for Syt-liposome binding determined from k_{obs}, as described in text. Data from three independent experiments. (D) Normalized plots of $K_{D\text{-}sf}$ and $K_{D\text{-}cs}$ (from Figure 5) versus PS content.

stability, PS could influence exocytosis at two or more sites, each through a different molecular mechanism.

The frequency of fusion events increased with cellular PS content, and this could reflect an acceleration of any kinetic step after Ca^{2+} entry up to fusion pore opening. Event frequency saturated at a PS content of ~15% (Figure 2A), and with PS confined to the inner leaflet of the plasma membrane, the PS content there should be ~30%. This saturation could reflect either the saturation of a PS-dependent binding process, a limiting pool of release-ready vesicles (Sorensen, 2004), or a change in the rate limiting step leading to pore opening. Regardless of the mechanism of saturation, the steep increase in event frequency at low PS parallels a steep increase in Syt I binding to liposomes at low PS (Figure 6D). This parallel is consistent with the view that Ca^{2+}-triggered binding of Syt I to membranes drives a step before or including fusion pore opening. However, as intriguing as this may be, the different values of PS content where this behavior was seen indicates that this parallel must be interpreted cautiously. Furthermore, it is possible that other PS-binding proteins show a qualitatively similar PS dependence of binding, and a number of other PS-binding proteins have roles in exocytosis (Stace and Ktistakis, 2006).

Table 2. Rate and binding constants for Syt I binding to liposomes containing various amounts of PS

PS	k_{on} (10^{10} M^{-1} s^{-1})	k_{off} ($^{-1}$)	$K_{D\text{-}sf}$ (nM)
9%	0.59 ± 0.11	64 ± 5	10.80 ± 3.70
12%	1.28 ± 0.08	36 ± 4	2.83 ± 0.52
15%	1.45 ± 0.17	29 ± 7	2.02 ± 0.81
25%	2.23 ± 0.15	10 ± 5	0.46 ± 0.29
35%	2.19 ± 0.11	9 ± 4	0.40 ± 0.23
45%	1.84 ± 0.19	12 ± 6	0.64 ± 0.46
55%	2.19 ± 0.15	12 ± 5	0.52 ± 0.29
95%	1.24 ± 0.13	8 ± 5	0.63 ± 0.52

The steep enhancement of Syt I binding to membranes with low PS content indicates a highly cooperative interaction, with PS molecules forming clusters as Syt I binds. The stoichiometry of Syt I liposome interactions suggests that one Syt I molecule binds to ~10 PS molecules in a lipid bilayer (Hui *et al.*, 2009). By contrast, the graded enhancement of binding at higher PS content may reflect a longer range electrostatic interaction between Syt I and bilayer surface charge, or an enhancement related to the high positive spontaneous curvature of PS (Fuller *et al.*, 2003).

Increasing PS levels stabilized open fusion pores. This effect was kinetically distinct from the increase in fusion event frequency. In contrast to the enhanced frequency, stabilizing fusion pores should reduce exocytosis. Fusion pores were stabilized primarily by a slower rate of pore dilation (Figure 4). Although enhancing fusion event frequency requires changing a kinetic process upstream from the open fusion pore, a parsimonious explanation that can account for both of these kinetic effects is that PS participates in an interaction that stabilizes open fusion pores. This stabilization would accelerate transitions into this state, to increase event frequency (Figure 2B), and decelerate transitions out of this state, to reduce k_d (Figure 4C). However, stabilizing fusion pores should also reduce the reverse process of pore closure (k_c), and this was not seen (Figure 4B).

To explore possible mechanisms for the involvement of Ca^{2+}-triggered Syt I binding to PS-containing membranes in exocytosis we envision a structural model for the fusion pore with complexes between Syt I and the inner face of the plasma membrane (Figure 7). When Ca^{2+} enters a cell it binds Syt I, which then binds membranes. The resulting penetration of bilayers (Chapman and Davis, 1998) could drive an inward dimpling of the membrane (Martens *et al.*, 2007; Hui *et al.*, 2009). This dimpling would allow the plasma membrane to protrude toward the vesicle to enable molecules in each membrane to interact and open a pore (Figure 7B). PS could also stabilize fusion pores by a mechanism independent of Syt I. PS is unusual among the major bio-

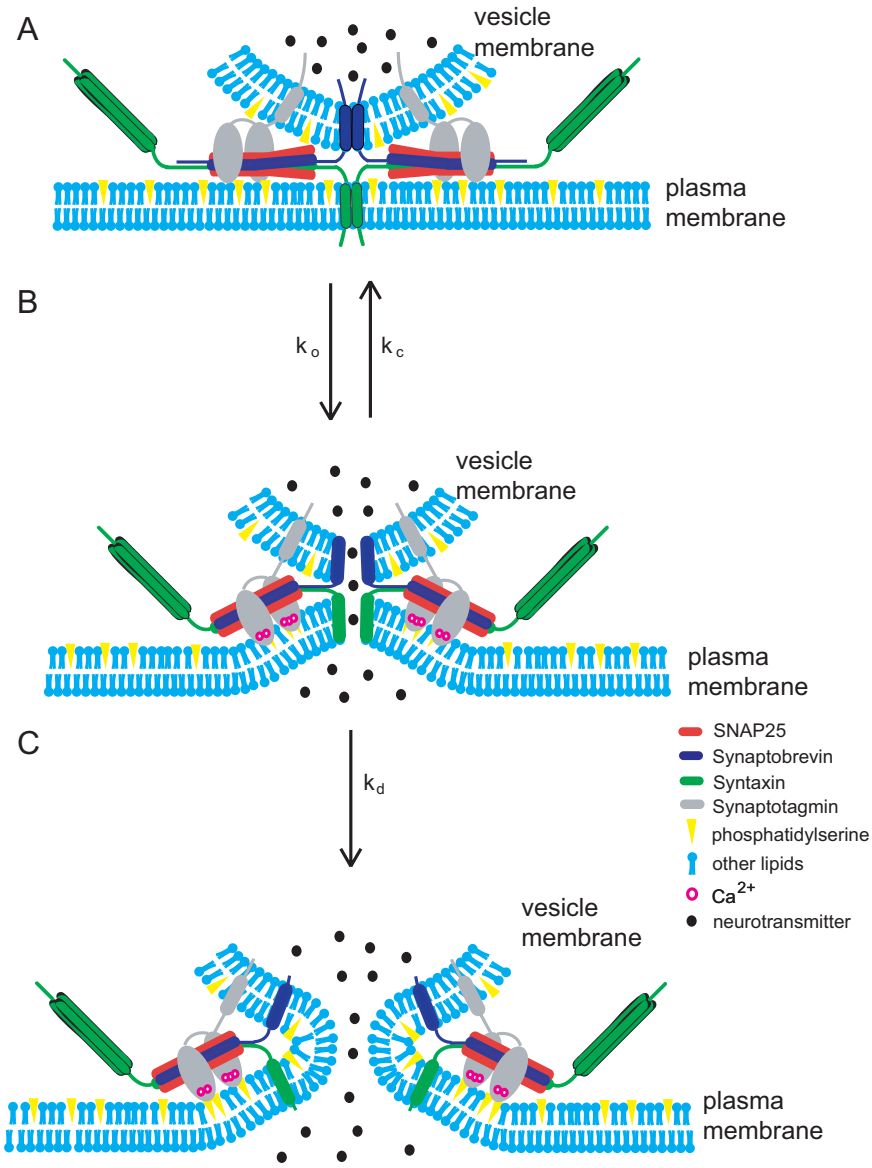

Figure 7. Models of PS interactions during exocytosis. (A) A release-ready vesicle before Ca^{2+} entry. (B) Ca^{2+} enters a cell and binds to Syt I. Syt I penetrates the plasma membrane, induces curvature, and pulls the plasma membrane fusion apparatus toward the vesicle to open a fusion pore. An open fusion pore can either close or dilate. (C) A lipidic fusion pore creates negative curvature in the PS-containing monolayer facing the cytoplasm. Note that with its inverted-cone shape, PS packs poorly into the inner leaflet of the lipid bilayer within the fusion pore.

logical phospholipids in having high positive spontaneous curvature (Fuller *et al*., 2003), and this has implications for PS stabilization of fusion pores. According to one hypothesis, the dilation of the fusion pore responsible for the PSF involves a transition from a proteinaceous pore to a lipidic pore (Han *et al*., 2004; Jackson and Chapman, 2008). The inner bilayer leaflet of a lipidic fusion pore has pronounced negative curvature, so that PS, with its positive spontaneous curvature, will not pack very well. Thus, increasing PS in the inner membrane leaflet will raise the energy cost of forming a lipidic pore (Figure 7C). PS could thus stabilize proteinaceous fusion pores by raising the energy for formation of the downstream state. An analysis of membrane curvature and fusion pore kinetics supports this interpretation (Zhang and Jackson, unpublished data). An important goal for future research is to design experiments that can distinguish between various alternative mechanisms by which PS can influence exocytosis.

Many proteins regulate fusion pores (Jackson and Chapman, 2006), but we know less about the effects of lipids (Uchiyama *et al*., 2007; Lam *et al*., 2008). In comparison with proteins, lipids are difficult to manipulate in living cells, due to the complex regulation of lipid-metabolizing enzymes (Vance and Vance, 2004). Here, we found ways to manipulate PS in cells to test its role in exocytosis. The negative charge of PS is clearly critical to its function in exocytosis, but PS also has unusually high positive spontaneous curvature (Fuller *et al*., 2003). This would promote inward protrusions or dimples (Figure 7B) but retard the evolution to a lipidic pore (Figure 7C). Deformations as pictured in Figure 7B also fit well with the ability of Syt I to bend membranes, and this will help lower the energy barrier for membrane fusion (Martens *et al*., 2007; Hui *et al*., 2009).

ACKNOWLEDGMENTS

We thank Dr. Jean Vance for providing PS synthase clones This work was funded by National Institutes of Health grants NS-44057 (to M.B.J.) and MH-61876 (to E.R.C.). E.R.C. is an investigator of the Howard Hughes Medical Institute.

REFERENCES

Amatore, C., Arbault, S., Bonifas, I., Bouret, Y., Erard, M., Ewing, A. G., and Sombers, L. A. (2005). Correlation between vesicle quantal size and fusion pore release in chromaffin cell exocytosis. Biophys. J. *88*, 4411–4420.

Augustine, G. J. (2001). How does calcium trigger neurotransmitter release? Curr. Opin. Neurobiol. *11*, 320–326.

Bai, J., Wang, C. T., Richards, D. A., Jackson, M. B., and Chapman, E. R. (2004). Fusion pore dynamics are regulated by synaptotagmin*t-SNARE interactions. Neuron *41*, 929–942.

Bai, J., Wang, P., and Chapman, E. R. (2002). C2A activates a cryptic Ca^{2+}-triggered membrane penetration activity within the C2B domain of synaptotagmin I. Proc. Natl. Acad. Sci. USA *99*, 1665–1670.

Bhalla, A., Tucker, W. C., and Chapman, E. R. (2005). Synaptotagmin isoforms couple distinct ranges of Ca2+, Ba2+, and Sr2+ concentration to SNARE-mediated membrane fusion. Mol. Biol. Cell *16*, 4755–4764.

Brose, N., Petrenko, A. G., Südhof, T. C., and Jahn, R. (1992). Synaptotagmin: a calcium sensor on the synaptic vesicle surface. Science *256*, 1021–1025.

Brunger, A. T. (2005). Structure and function of SNARE and SNARE-interacting proteins. Q. Rev. Biophys. *38*, 1–47.

Chapman, E. R. (2002). Synaptotagmin: a Ca(2+) sensor that triggers exocytosis? Nat. Rev. Mol. Cell Biol. *3*, 498–508.

Chapman, E. R., and Davis, A. (1998). Direct interaction of a Ca^{2+}-binding loop of synaptotagmin with lipid bilayers. J. Biol. Chem. *273*, 13995–14001.

Daleke, D. L. (2003). Regulation of transbilayer plasma membrane phospholipid asymmetry. J. Lipid. Res. *44*, 233–242.

Fernandez-Chacon, R., Konigstorfer, A., Gerber, S. H., Garcia, J., Matos, M. F., Stevens, C. F., Brose, N., Rizo, J., Rosenmund, C., and Sudhof, T. C. (2001). Synaptotagmin I functions as a calcium regulator of release probability. Nature *410*, 41–49.

Fernandez-Chacon, R., Shin, O. H., Konigstorfer, A., Matos, M. F., Meyer, A. C., Garcia, J., Gerber, S. H., Rizo, J., Sudhof, T. C., and Rosenmund, C. (2002). Structure/function analysis of Ca2+ binding to the C2A domain of synaptotagmin 1. J. Neurosci. *22*, 8438–8446.

Folch, J., Lees, M., and Sloane Stanley, G. H. (1957). A simple method for the isolation and purification of total lipides from animal tissues. J. Biol. Chem. *226*, 497–509.

Fuller, N., Benatti, C. R., and Rand, R. P. (2003). Curvature and bending constants for phosphatidylserine-containing membranes. Biophys. J. *85*, 1667–1674.

Han, X., and Jackson, M. B. (2006). Structural transitions in the synaptic SNARE complex during Ca2+-triggered exocytosis. J. Cell Biol. *172*, 281–293.

Han, X., Wang, C. T., Bai, J., Chapman, E. R., and Jackson, M. B. (2004). Transmembrane segments of syntaxin line the fusion pore of Ca2+-triggered exocytosis. Science *304*, 289–292.

Hui, E., Johnson, C. P., Yao, J., Dunning, F. M., and Chapman, E. R. (2009). Protein mediated membrane bending is a common critical step in membrane fusion and fission. Cell *138*, 709–721.

Jackson, M. B., and Chapman, E. R. (2006). Fusion pores and fusion machines in Ca2+-triggered exocytosis. Annu. Rev. Biophys. Biomol. Struct. *35*, 135–160.

Jackson, M. B., and Chapman, E. R. (2008). The fusion pores of Ca(2+)-triggered exocytosis. Nat. Struct. Mol. Biol. *15*, 684–689.

Jahn, R., and Scheller, R. H. (2006). SNAREs–engines for membrane fusion. Nat. Rev. Mol. Cell Biol. *7*, 631–643.

Koh, T. W., and Bellen, H. J. (2003). Synaptotagmin I, a Ca^{2+} sensor for neurotransmitter release. Trends Neurosci. *26*, 413–422.

Kuge, O., and Nishijima, M. (2003). Biosynthetic regulation and intracellular transport of phosphatidylserine in mammalian cells. J. Biochem. *133*, 397–403.

Kuge, O., Nishijima, M., and Akamatsu, Y. (1985). Isolation of a somatic-cell mutant defective in phosphatidylserine biosynthesis. Proc. Natl. Acad. Sci. USA *82*, 1926–1930.

Kuge, O., Saito, K., and Nishijima, M. (1997). Cloning of a Chinese hamster ovary (CHO) cDNA encoding phosphatidylserine synthase (PSS) II, overexpression of which suppresses the phosphatidylserine biosynthetic defect of a PSS I-lacking mutant of CHO-K1 cells. J. Biol. Chem. *272*, 19133–19139.

Lam, A. D., Tryoen-Toth, P., Tsai, B., Vitale, N., and Stuenkel, E. L. (2008). SNARE-catalyzed fusion events are regulated by syntaxin1a-lipid interactions. Mol. Biol. Cell *19*, 485–497.

Lynch, K. L., Gerona, R. R., Kielar, D. M., Martens, S., McMahon, H. T., and Martin, T. F. (2008). Synaptotagmin-1 utilizes membrane bending and SNARE binding to drive fusion pore expansion. Mol. Biol. Cell *19*, 5093–5103.

Mackler, J. M., Drummond, J. A., Loewen, C. A., Robinson, I. M., and Reist, N. E. (2002). The C(2)B Ca(2+)-binding motif of synaptotagmin is required for synaptic transmission in vivo. Nature *418*, 340–344.

Martens, S., Kozlov, M. M., and McMahon, H. T. (2007). How synaptotagmin promotes membrane fusion. Science *316*, 1205–1208.

Nagy, G., Kim, J. H., Pang, Z. P., Matti, U., Rettig, J., Sudhof, T. C., and Sorensen, J. B. (2006). Different effects on fast exocytosis induced by synaptotagmin 1 and 2 isoforms and abundance but not by phosphorylation. J. Neurosci. *26*, 632–643.

Nishiki, T., and Augustine, G. J. (2004). Dual roles of the C2B domain of synaptotagmin I in synchronizing Ca2+-dependent neurotransmitter release. J. Neurosci. *24*, 8542–8550.

Paddock, B. E., Striegel, A. R., Hui, E., Chapman, E. R., and Reist, N. E. (2008). Ca2+-dependent, phospholipid-binding residues of synaptotagmin are critical for excitation-secretion coupling in vivo. J. Neurosci. *28*, 7458–7466.

Pang, Z. P., Shin, O. H., Meyer, A. C., Rosenmund, C., and Sudhof, T. C. (2006). A gain-of-function mutation in synaptotagmin-1 reveals a critical role of Ca2+-dependent soluble N-ethylmaleimide-sensitive factor attachment protein receptor complex binding in synaptic exocytosis. J. Neurosci. *26*, 12556–12565.

Perkins, R. G., and Scott, R. E. (1978). Differences in the phospholipid, cholesterol, and fatty acyl composition of 3T3 and SV3T3 plasma membranes. Lipids *13*, 653–657.

Pomorski, T., Hrafnsdottir, S., Devaux, P. F., and van Meer, G. (2001). Lipid distribution and transport across cellular membranes. Semin. Cell Dev. Biol. *12*, 139–148.

Saito, K., Nishijima, M., and Kuge, O. (1998). Genetic evidence that phosphatidylserine synthase II catalyzes the conversion of phosphatidylethanolamine to phosphatidylserine in Chinese hamster ovary cells. J. Biol. Chem. *273*, 17199–17205.

Scott, R. E. (1976). Plasma membrane vesiculation: a new technique for isolation of plasma membranes. Science *194*, 743–745.

Sollner, T., Whiteheart, S. W., Brunner, M., Erdjument-Bromage, H., Geromanos, S., Tempst, P., and Rothman, J. E. (1993). SNAP receptors implicated in vesicle targeting and fusion. Nature *362*, 318–324.

Sombers, L. A., Hanchar, H. J., Colliver, T. L., Wittenberg, N., Cans, A., Arbault, S., Amatore, C., and Ewing, A. G. (2004). The effects of vesicular volume on secretion through the fusion pore in exocytotic release from PC12 cells. J. Neurosci. *24*, 303–309.

Sorensen, J. B. (2004). Formation, stabilisation and fusion of the readily releasable pool of secretory vesicles. Pflugers Arch. *448*, 347–362.

Stace, C. L., and Ktistakis, N. T. (2006). Phosphatidic acid- and phosphatidylserine-binding proteins. Biochim. Biophys. Acta *1761*, 913–926.

Stevens, C. F., and Sullivan, J. M. (2003). The synaptotagmin C2A domain is part of the calcium sensor controlling fast synaptic transmission. Neuron *39*, 299–308.

Tucker, W. C., Edwardson, J. M., Bai, J., Kim, H. J., Martin, T. F., and Chapman, E. R. (2003). Identification of synaptotagmin effectors via acute inhibition of secretion from cracked PC12 cells. J. Cell Biol. *162*, 199–209.

Ubach, J., Lao, Y., Fernandez, I., Arac, D., Sudhof, T. C., and Rizo, J. (2001). The C2B domain of synaptotagmin I is a Ca2+-binding module. Biochemistry *40*, 5854–5860.

Uchiyama, Y., Maxson, M. M., Sawada, T., Nakano, A., and Ewing, A. G. (2007). Phospholipid mediated plasticity in exocytosis observed in PC12 cells. Brain Res. *1151*, 46–54.

Van Kessel, W. S., Hax, W. M., Demel, R. A., and De Gier, J. (1977). High performance liquid chromatographic separation and direct ultraviolet detection of phospholipids. Biochim. Biophys. Acta *486*, 524–530.

Vance, J. E., and Vance, D. E. (2004). Phospholipid biosynthesis in mammalian cells. Biochem. Cell Biol. *82*, 113–128.

Voelker, D. R., and Frazier, J. L. (1986). Isolation and characterization of a Chinese hamster ovary cell line requiring ethanolamine or phosphatidylserine for growth and exhibiting defective phosphatidylserine synthase activity. J. Biol. Chem. *261*, 1002–1008.

Wang, C. T., Bai, J., Chang, P. Y., Chapman, E. R., and Jackson, M. B. (2006). Synaptotagmin-Ca2+ triggers two sequential steps in regulated exocytosis in

rat PC12 cells: fusion pore opening and fusion pore dilation. J. Physiol. *570*, 295–307.

Wang, C. T., Grishanin, R., Earles, C. A., Chang, P. Y., Martin, T. F., Chapman, E. R., and Jackson, M. B. (2001). Synaptotagmin modulation of fusion pore kinetics in regulated exocytosis of dense-core vesicles. Science *294*, 1111–1115.

Wang, C. T., Lu, J. C., Bai, J., Chang, P. Y., Martin, T. F., Chapman, E. R., and Jackson, M. B. (2003a). Different domains of synaptotagmin control the choice between kiss-and-run and full fusion. Nature *424*, 943–947.

Wang, P., Wang, C. T., Bai, J., Jackson, M. B., and Chapman, E. R. (2003b). Mutations in the effector binding loops in the C2A and C2B domains of synaptotagmin I disrupt exocytosis in a non-additive manner. J. Biol. Chem. *278*, 47030–47037.

Yeung, T., Terebiznik, M., Yu, L., Silvius, J., Abidi, W. M., Philips, M., Levine, T., Kapus, A., and Grinstein, S. (2006). Receptor activation alters inner surface potential during phagocytosis. Science *313*, 347–351.

Zhang, Z., and Jackson, M. B. (2008). Temperature dependence of fusion kinetics and fusion pores in Ca2+-triggered exocytosis from PC12 cells. J. Gen. Physiol. *131*, 117–124.

Zwaal, R. F., Comfurius, P., and Bevers, E. M. (2005). Surface exposure of phosphatidylserine in pathological cells. Cell Mol. Life Sci. *62*, 971–988.